Magnetic and transport properties in ordered arrays of permalloy antidots and thin films

G. A. Badini Confalonieri, K. R. Pirota, M. Vazquez, N. M. Nemes, M. Garcia-Hernandez et al.

Citation: J. Appl. Phys. **107**, 083918 (2010); doi: 10.1063/1.3383039
View online: http://dx.doi.org/10.1063/1.3383039
View Table of Contents: http://jap.aip.org/resource/1/JAPIAU/v107/i8
Published by the AIP Publishing LLC.

Magnetic and transport properties in ordered arrays of permalloy antidots and thin films

G. A. Badini Confalonieri,[1,a)] K. R. Pirota,[2] M. Vazquez,[1] N. M. Nemes,[1] M. Garcia-Hernandez,[1] M. Knobel,[2] and F. Batallan[1]
[1]*Instituto de Ciencia de Materiales de Madrid, Campus de Cantoblanco, 28049 Madrid, Spain*
[2]*"Gleb Wataghin" (IFGW), Universidade Estadual de Campinas (UNICAMP), C.P. 6165, 13.083-970 Campinas S.P., Brazil*

(Received 2 October 2009; accepted 10 March 2010; published online 29 April 2010)

The magnetotransport behaviors of two types of permalloy nanostructures, thin films and antidots, are presented and discussed. Antidots samples were prepared by sputtering a $Ni_{80}Fe_{20}$ layer on top of a nanoporous alumina membrane. A counterpart continuous thin film grown on a continuous Si substrate was also prepared. The magnetoresistance (MR) was measured both as a function of the external applied magnetic field and of the angular orientation, and thus compared with the magnetization curves. The introduction of antidots is found to reduce the anisotropic MR and the angular dependence of the MR, simultaneously increasing the coercive field of the samples. The influence of the sample geometry on the perpendicular MR behavior is reported and discussed.
 [doi:10.1063/1.3383039]

I. INTRODUCTION

The interest of the scientific community on magnetic nanostructures experienced a continuous increase over the last years thanks to the high potential of these materials in many technological applications, as well as for the study of several fundamental properties.

Among these systems, arrays of periodic holes in a thin film, known as antidots, have been the subject of many studies,[1–4] since the use of antidots induces a strong shape anisotropy in the film, which, in turn, allows the control of magnetic properties such as magnetoresistance (MR), coercivity, permeability, and magnetization reversal.[5–7] In particular, several research groups reported interesting data of magnetic, transport, and dynamic properties in ordered arrays of permalloy antidots, covering a wide range of geometrical parameters. Antidot systems are usually prepared in the micron or submicron scale by lithographic techniques[3,8] or using block copolymers templates.[9] More recently, ordered arrays of antidots have been prepared by growing a magnetic thin film on top of a nanoporous alumina membrane (NAM) substrates.[1,10–12] In the present study, this method was chosen to prepare permalloy antidots with a pore size below 100 nm and very stable lattice parameters over a sample area of several square millimeters, something otherwise difficult to achieve with conventional lithographic techniques. The magnetic and transport properties of these systems are presented and compared with counterpart continuous thin film samples.

II. EXPERIMENTAL METHODS

Magnetic thin films and antidots were fabricated by depositing $Fe_{20}Ni_{80}$ by ion beam sputtering on top of a Si and NAM substrates, respectively. The energy and total current for the sputter ion gun were 500 eV and 10 mA, respectively, giving a deposition rate of ~0.3 Å/s controlled by a quartz crystal monitor. The base pressure before deposition was 2×10^{-7} Torr. During the deposition process, the substrate temperature was kept at 200 °C. The $Fe_{20}Ni_{80}$ layer has a total thickness of 80 nm. The samples were capped with 3 nm Cu layer to prevent oxidation of the magnetic layer for "*ex situ*" characterization.

In the case of the antidot structure, the obtained $Fe_{20}Ni_{80}$ film perfectly replicated the well-ordered array of nanoholes of the substrate resulting in a film with arrays of antidots. The NAMs were fabricated using a two-step anodization process[12] in oxalic acid. The initial pore diameter, $d = 35$ nm, and intrapore spacing, $D = 105$ nm, were controlled by choosing appropriate anodization conditions. The pores were enlarged by a subsequent heat treatment in phosphoric acid (5% in volume) at 35 °C with a rate of 2 nm/min, to a total diameter of 95 nm, whereas the distance between the centers of the pores, D, was kept constant.[12] After sputtering of the $Fe_{20}Ni_{80}$ layer the pore diameter was reduced to 80 ± 2 nm, as shown in Fig. 1. In all cases, the membranes show a high hexagonal order and a good uniformity on both size and distance between pores.

MR was measured with a quantum design physical properties measurement system with an applied field, H, up to 80 kOe. The system has a rotating probe that allows the rotation of the sample, relative to the applied field direction, with a step angle of 0.1°. In this study, a four probe resistance measurement was used, the sample plane defining the xy plane, where current and voltage were injected and measured, respectively, in the x direction. The magnetic field direction varies in the zx plane, θ being the angle between H and the xy plane. Therefore, $R_{\parallel}$ indicates the MR measurement with H parallel to the x direction while $R_{\perp}$ indicates H parallel to the z direction.

a)Electronic mail: gabadinic@yahoo.com.

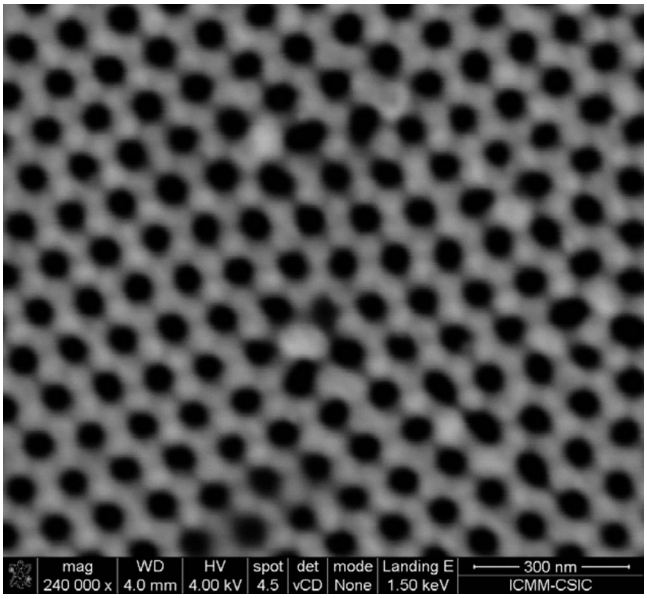

FIG. 1. Scanning electron microscopy (SEM) image of a 80 nm thick permalloy antidots film grown on top of a NAM.

Magnetization curves were measured by means of a vibrating sample magnetometer. All measurements were performed at room temperature.

III. RESULTS AND DISCUSSION

The transport properties in ferromagnetic metals are a consequence of the symmetry properties of the ferromagnetic state. To describe the resistivity tensor, $\rho_{ij}(B)$, we need three different components: $\rho_{\parallel}(B)$, $\rho_{\perp}(B)$, and $\rho_H(B)$. The three components depend on the magnetic induction B, which is a function of the external field, the magnetization, and the demagnetising factor D of the particular sample geometry: $B=H+4\pi M(1-D)$.

Conventionally, the coefficients $\rho_{ij}(B)$ are split up into two parts $\rho_{ij}(B)=\rho_{ij}^0(B)+\rho_{ij}^s(B)$ where $\rho_{ij}^0(B)$ are the ordinary coefficients, and, $\rho_{ij}^s(B)$, are the spontaneous or extraordinary coefficients. In practice, extrapolating the high magnetic field value of $\rho_{ij}(B)$ to $B=0$, three spontaneous parameters independent of B are obtained: $\rho_{\parallel}$, $\rho_{\perp}$, and ρ_H. The fact that the two elements $\rho_{\parallel}$ and $\rho_{\perp}$ are unequal means that the resistivity depends on the relative orientation of M and the current density, J.[13] It is, therefore, important to identify the exact parallel and perpendicular geometries for the proposed experimental setup. Figure 2 shows the angular dependence of the resistance for the thin film and the antidots samples, at an applied field of 1 kOe. Both samples are characterized by an abrupt change in R and the angle at which the minimum of the curve is found, namely 90°, is taken as $R_{\perp}$.[14] This effect is known as anisotropic MR (AMR) and it will be further discussed in the following sections. When comparing Figs. 2(a) and 2(b), it is possible to appreciate an increase by a factor of 10 in the measured value of R, from the thin film to the antidots sample. This can be better understood considering changes in the geometry as well as in the magnetic structure of the sample. The introduction of hexagonal antidots in the structure, with three antidots per hexagonal unit cell, reduces the volume of the unit cell to 53% of its original volume and thus increasing the resistance of the material. Moreover, it should be remembered that around the antidots, a stable domain configuration is formed which is a result of the interplay of intrinsic uniaxial anisotropy of the magnetic thin film and the local demagnetizing fields associated with the antidots.[15] The change in R is, therefore, due to intrinsic structural modifications, of both geometrical and magnetic origin.

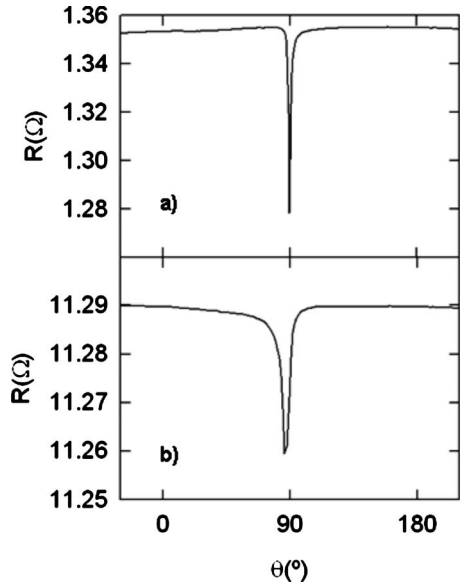

FIG. 2. Angular variation in R for the (a) thin film and (b) antidots samples. Both samples are characterized by an abrupt change in R around 90°, where the minimum is found. As can be seen, there is a change of about 5.4% for the continuous film and 0.2% for the antidot arrays.

It is worth noting that large difference between the relative changes in resistance between 0 and 90° found for the two samples. While for the continuous thin film this change is approximately 5.4%, for the antidot arrays this value decreases down to 0.2%. This effect reveals a considerable decrease in the anisotropy due to the introduction of the pores.

The MR curves and the magnetic hysteresis loops for the antidots array and the thin film samples are presented in Figs. 3 and 4, respectively. Both samples were measured in the parallel and perpendicular directions. The $R_{\parallel}$ [Figs. 3(a) and 4(a)] and $R_{\perp}$ [Figs. 3(c) and 4(c)] curves are characterized

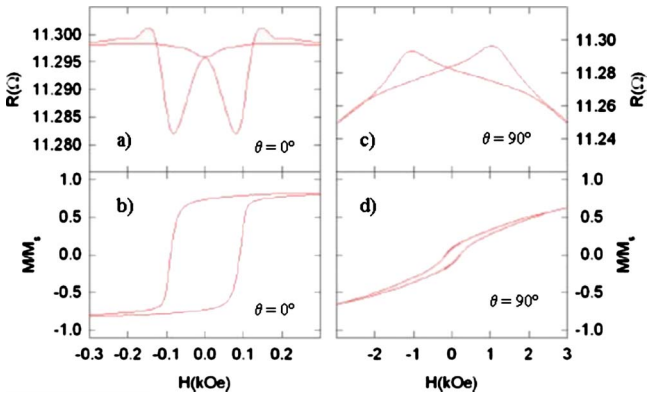

FIG. 3. (Color online) Low field $R_{\parallel}$ and $R_{\perp}$ compared with the respective magnetization curves for the antidots array sample.

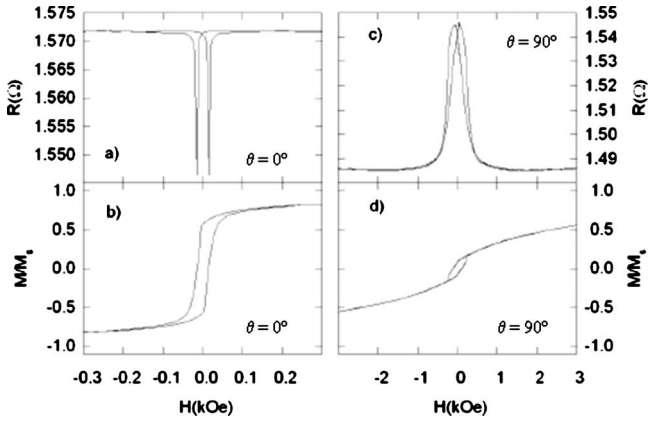

FIG. 4. Low field $R_{\parallel}$ and $R_{\perp}$ compared with the respective magnetization curves for the thin film sample.

by sharp peaks at low values of applied magnetic fields. The normalized magnetization curves are presented in Figs. 3(b) and 3(d) and Figs. 4(b) and 4(d) for the antidots array and thin film samples, respectively. In both cases, the samples easy axis is found to lay in the plane of the film. The introduction of antidots substantially modifies the permalloy properties, increasing the coercivity, H_c, by a factor of 10. This should be ascribed to the enhanced pinning mechanism for the existing walls to propagate. In fact, in these magnetic nanostructures, the reversal occurs by the movement of domain walls through the film, and the pinning at the antidots leads to the enhanced coercivity, compared with the continuous film.[16] The enhancement in coercivity can, in part, also be attributed by the roughness of the alumina substrate, estimated to be in the range of approximately 10–15 nm (Ref. 17); in fact, irregularities in the interphase between the magnetic thin films and the alumina substrate can act as pinning sites against the propagation of magnetic domain walls. Comparing the magnetization curves with the MR curves, it is found that the peaks of the MR curves correspond to the coming out of saturation of the samples, where irreversible magnetization processes take place. This suggests that the peaks should be associated with magnetic domain formations and domain wall nucleation and displacement, where large changes of M over small increment of H can be observed. This also explains why these features are found at higher fields for the antidots array sample when compared with the thin film counterpart.

The high field perpendicular MR curves, shown in Fig. 5, are characterized by a parabolic behavior, the ends of the parabola coinciding with the magnetic saturation of the sample. Interestingly, however, the parabola of the thin film has an opposite curvature to that of the antidots array sample. In the $R_{\perp}$ curves, measured up to 2 T, three different regions can be identified:

(1) The high magnetic field region, for $H_s < H$, where H_s, the saturating field, is characterized by a linear behavior.
(2) The parabolic region, defined by $H < H_s$, where R(H) has a parabolic behavior.
(3) The irreversibility region, defined by $H < H_I$, corresponding to the central region around H=0, where H_I, the irreversibility field, is defined as the maximum field where the value of the measured R(H) presents some hysteresis (i.e., measurements performed with increasing fields are different from the ones obtained with decreasing field).

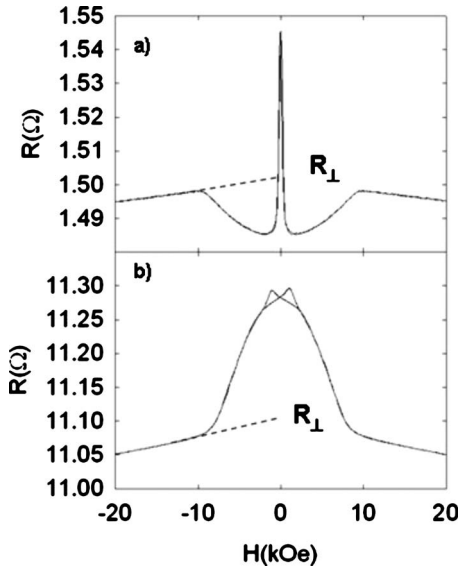

FIG. 5. $R_{\perp}$ for (a) thin film and (b) antidots array samples. The high field region extrapolated at H=0 is shown by the dashed line.

The high field region has a negative slope that is attributed to the increase in magnetization or spin order through the high field susceptibility and the applied field. This high field susceptibility effect overcomes the ordinary electronic MR that, in turn, is positive. This region can be used to calculate the AMR ratio, $\Delta R/R_{ave}$, that is a measurement of the difference in resistance when the magnetization vector of a single domain ferromagnet in zero field lays either parallel or perpendicular to the current.[18] $\Delta R/R_{ave}$, is given by the following equation:[18]

$$\frac{\Delta R}{R_{ave}} = \frac{R_{\parallel} - R_{\perp}}{(R_{\parallel} + 2R_{\perp})/3}, \tag{1}$$

where $R_{\parallel}$ and $R_{\perp}$ are the resistance values conveniently extrapolated to B=0 as shown in Fig. 5. From a practical point of view, B=0 is not easily defined because of the difficulty to obtain the demagnetising field, therefore, $R_{\parallel}$ and $R_{\perp}$ are extrapolated to H=0, the difference being, in this case, negligible.

In the case of the thin film, the value of AMR is 4.7%, which is consistent with previous values reported in the literature.[18] On the other hand, the antidot array sample display a value of 1.8%, further indicating that the antidots lead to a reduction in the anisotropy of the system.

A detailed study of the MR at, and around, θ=90° is presented in Figs. 6(a) and 6(b), for the thin film and antidots arrays amples, respectively. Figure 6(a), measured with a minimum step angle of 0.5° show a considerable difference between the curve obtained exactly at 90° and its neighboring curves. At 90°, a negative magnetoresistive parabolic behavior is observed, i.e., the resistance decreases below the saturation values, as already reported in Fig. 5. This shows the extreme sensitivity to θ of the MR response. This result

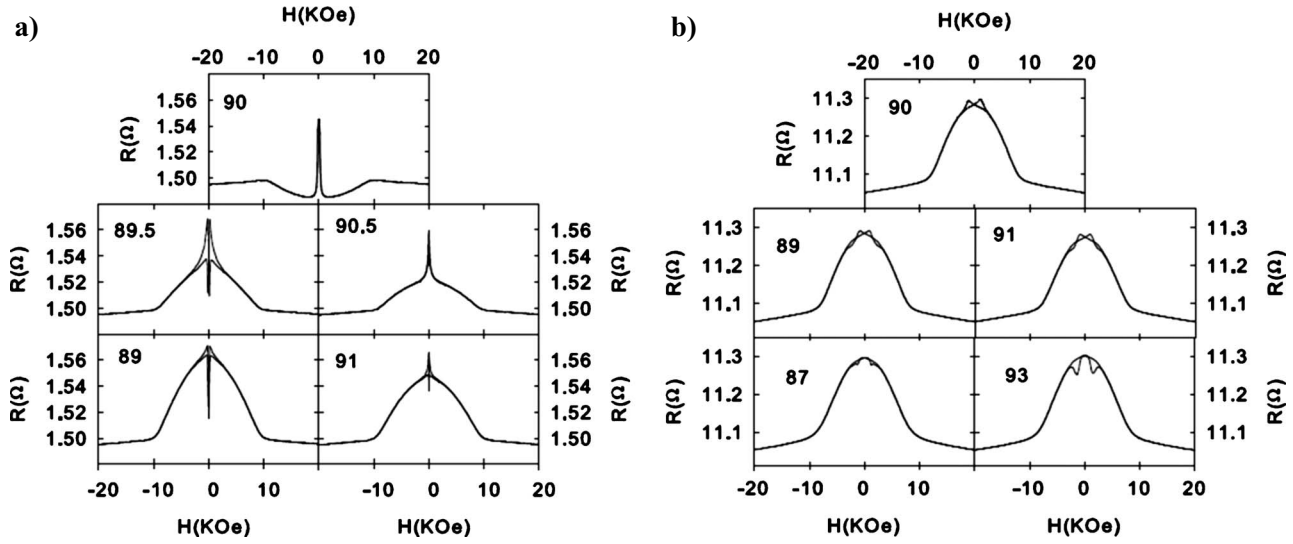

FIG. 6. The MR behavior at and around $\theta=90°$ for both the (a) thin film and (b) antidots array samples.

does not agree with previously reported results on MR measured in permalloy thin films,[19–21] nanowires,[22,23] nanodots,[24] and square-shaped antidots.[25] A possible reason could be the difficulty, in many experimental systems, to identify the exact position of a perpendicular direction with a precision of 0.5° or less. Moreover, we cannot exclude that this behavior could be thickness dependent and related to the existence of a stripe domain structure.[26] For angles other than 90°, in the range between 83° and 97°, the observed MR curves show a positive parabolic behavior, similar to the results reported in the above cited works. In the case of antidots array sample the MR response, shown in Fig. 5(b) (measured in the same conditions as used for the continuous film) studied with a minimum step angle of 1°, is substantially different, the thin film showing an abrupt change at $\theta=90°$ and having higher angular dependence. The difference between the two samples can be explained in terms of changes in the shape anisotropy, internal domain structures, and the pinning of domains wall exerted by the antidots as explained in connection with the magnetization measurements shown in Figs. 3 and 4.

It is also worth noticing that for both samples, the MR curves in the range of angles considered, is not symmetric around 90°, showing slightly different response depending on whether the sample is measured either for angles larger than 90° or smaller. This is also related to the asymmetric shape of the minimum observed in Fig. 2, reflecting different magnetization behaviors before and after 90°. This trend is attributed to the presence of an intrinsic anisotropy in the basal plane of the samples. Furthermore, the presence of a dead layer between the substrate and the film, arising from oxidation of the film during the sputtering process, could also account for the observed asymmetry.

IV. CONCLUSIONS

The magnetization and transport properties of array of permalloy antidots were studied and compared with a continuous thin film counterpart sample using an extremely precise angular controller. The introduction of the period array of pores is found to substantially modify the anisotropy of the film that is directly observed in the MR measurements. Both the resistance and the coercivity of the antidots are found to increase by a factor of 10 due to change in the geometrical current path and the magnetic domain structure, with the antidots acting as pinning sites during domain wall movement. Anomalous negative behavior of $R_{\perp}$ for the thin film sample was observed to be extremely sensitive to the measuring angles, probably due to the refined angular control between the sample magnetization and the applied current.

[1] Y. G. Ma, S. L. Limand, and C. K. Ong, J. Phys. D **40**, 935 (2007).
[2] S. Martens, O. Albrecht, K. Nielsch, and D. Görlitza, J. Appl. Phys. **105**, 07C113 (2009).
[3] C. C. Wang, A. O. Adeyeye, N. Singh, Y. S. Huang, and Y. H. Wu, Phys. Rev. B **72**, 174426 (2005).
[4] C. T. Yu, H. Jiang, L. Shen, P. J. Flanders, and G. J. Mankey, J. Appl. Phys. **87**, 6322 (2000).
[5] N. Singh, S. Goolaup, and A. O. Adeyeye, Nanotechnology **15**, 1539 (2004).
[6] C. Y. Han, Z. L. Xiao, H. H. Wang, G. A. Willing, U. Geiser, U. Welp, W. K. Kwok, S. D. Bader, and G. W. Crabtree, Plating and Surface Finishing **91**, 40 (2004).
[7] W. Y. Lee, H. T. Leung, W. Zhang, Y. B. Xu, A. Hirohata, C. C. Yao, B.-Ch. Choi, D. G. Hasko, and J. A. C. Bland, IEEE Trans. Magn. **35**, 3475 (1999).
[8] C. C. Wang, A. O. Adeyeye, and N. Singh, Nanotechnology **17**, 1629 (2006).
[9] V. P. Chuang, W. Jung, C. A. Ross, J. Y. Cheng, O.-H. Park, and H.-C. Kim, J. Appl. Phys. **103**, 074307 (2008).
[10] Z. L. Xiao, C. Y. Han, U. Welp, H. H. Wang, V. K. Vlasko-Vlasov, W. K. Kwok, D. J. Miller, J. M. Hiller, R. E. Cook, G. A. Willing, and G. W. Crabtree, Appl. Phys. Lett. **81**, 2869 (2002).
[11] D. Navas, F. Ilievski, and C. A. Ross, J. Appl. Phys. **105**, 113921 (2009).
[12] K. R. Pirota, P. Prieto, A. M. J. Netob, J. M. Sanz, M. Knobel, and M. Vázquez, J. Magn. Magn. Mater. **320**, e235 (2008).
[13] I. A. Campbell and A. Fert, in *Ferromagnetic Materials*, edited by E. P. Wohlfarth (North-Holland, Amsterdam, 1982), Vol. 3.
[14] W. Döring, Ann. Phys. **424**, 259 (1938).
[15] M. Jaafar, D. Navas, A. Asenjo, M. Vazquez, M. Hernandez-Velez, and J. M. Garcia-Martin, J Appl. Phys., **101**, 09F513 (2007).
[16] F. J. Castaño, K. Nielsh, C. A. Ross, J. W. A. Robinson, and R. Krishnan, Appl. Phys. Lett. **85**, 2872 (2004).
[17] D. C. Leitao, C. T. Sousa, J. Ventura, F. Carpinteiro, J. G. Correia, M. M. Amado, J. B. Sousa, and J. P. Araujo, Phys. Status Solidi C **5**, 3488 (2008).
[18] T. R. McGuire and R. I. Potter, IEEE Trans. Magn. **11**, 1018 (1975).
[19] S. K. Decker and C. Tsang, IEEE Trans. Magn. **16**, 643 (1980).

[20]J. P. J. Groenland, C. J. M. Eijkel, J. H. J. Flultman, and R. M. de Ridder, Sens. Actuators, A **30**, 89 (1992).
[21]N. García, C. Hao, L. Yonghua, M. Muñoza, Y. Chen, Z. Cui, Z. Lu, Y. Zhou, G. Pan, and A. A. Pasa, Appl. Phys. Lett. **89**, 083112 (2006).
[22]J. L. Tsai, S. F. Lee, Y. D. Yao, C. Yu, and S. H. Liou, J. Appl. Phys. **91**, 10 (2002).
[23]T. Y. Chung and S. Y. Hsu, J. Appl. Phys. **103**, 07C506 (2008).
[24]T. Y. Chung and S. Y. Hsu, J. Appl. Phys. **99**, 08B707 (2006).
[25]A. O. Adeyeye, J. A. C. Bland, and C. Daboo, Appl. Phys. Lett. **70**, 3164 (1997).
[26]C. A. Ramos, E. VassalloBrigneti, J. Gomez, and A. Butera, Physica B **404**, 2784 (2009).